Atmospheric
Chemistry
and Physics
Discussions

Sensitivity of the tropical stratospheric ozone response to the solar rotational cycle in observations and chemistry-climate model simulations

Rémi Thiéblemont[1], Marion Marchand[1], Slimane Bekki[1], Sébastien Bossay[1], Franck Lefèvre[1], Mustapha Meftah[1], Alain Hauchecorne[1]

[1]Laboratoire, Milieux, Observations Spatiales, Institut Pierre Simon Laplace, CNRS, Paris, France.

Correspondence to: Rémi Thiéblemont (remi.thieblemont@latmos.ipsl.fr)

Abstract. The tropical stratospheric ozone response to solar UV variations associated with the rotational cycle (~27 days) is analysed using MLS satellite observations and numerical simulations from the LMDz-Reprobus chemistry-climate model. The model is used in two configurations, as a chemistry-transport model (CTM) where dynamics are nudged toward ERA-Interim reanalysis and as a chemistry-climate model (free-running) (CCM). An ensemble of five 17year simulations (1991-2007) is performed with the CCM. All simulations are forced by reconstructed time-varying solar spectral irradiance from the Naval Research Laboratory Solar Spectral Irradiance model. We first examine the ozone response to the solar rotational cycle during two 3year periods which correspond to the declining phases of solar cycle 22 (10/1991-09/1994) and solar cycle 23 (09/2004-08/2007) when the satellite ozone observations of the two Microwave Limb Sounders (MLS-UARS and MLS-Aura) are available. In the observations, during the first period, ozone and UV flux are found to be correlated between about 10 and 1 hPa with a maximum of 0.29 at ~5 hPa; the ozone sensitivity (% change in ozone for 1% change in UV) peaks at ~0.4. Correlation during the second period is weaker and has a peak ozone sensitivity of only 0.2, possibly due to the fact that the solar forcing is weaker during that period. The CTM simulation reproduces most of these observed features, including the differences between the two periods. The CCM ensemble mean results comparatively show much smaller differences between the two periods, suggesting that the amplitude of the rotational ozone signal estimated from MLS observations or the CTM simulation is strongly influenced by other (non-solar) sources of variability, notably dynamics. The analysis of the ensemble of CCM simulations shows that the estimation of the ensemble mean ozone sensitivity does not vary significantly neither with the amplitude of the solar rotational fluctuations, nor with the size of the time window used for the ozone sensitivity retrieval. In contrast, the uncertainty of the ozone sensitivity estimate significantly increases during periods of decreasing amplitude of solar rotational fluctuations (also coinciding with minimum phases of the solar cycle), and for decreasing size of the time window analysis. We found that a minimum of 3year and 10year time window is needed for the 1σ uncertainty to drop below 50% and 20%, respectively. These uncertainty sources may explain some of the discrepancies found in previous estimates of the ozone response to the solar rotational cycle.

1 Introduction

The thermal structure and the composition of the middle atmosphere are sensitive to fluctuations in the incoming solar radiation, which in turn can affect the Earth's surface climate variability (Gray et al., 2010). These solar variations are dominated by the 11year solar magnetic activity cycle and the solar rotational cycle, also called 27day solar cycle. Changes in

5 total solar irradiance (TSI) over an 11year solar cycle are typically lower than 0.1%, that correspond to 1 W m^{-2} change for a reference value of 1360.8 ± 0.5 W m^{-2} (Kopp and Lean, 2011). Such small variations in the total energy input are not expected to have a significant impact on climate, compared for instance to the variations of anthropogenic origin, and thus air-sea coupling mechanisms have been proposed that act to amplify the small solar initial perturbations (e.g. Meehl et al., 2008). Another possible amplification mechanism, also known as "top-down" (Kodera and Kuroda, 2002), operates through changes

10 in the spectral solar irradiance (SSI) - in particular in the ultraviolet (UV) range - that directly modulate the stratospheric temperatures and ozone concentrations. These perturbations induce dynamical changes in the stratosphere, which may in turn affect the tropospheric circulation through stratosphere-troposphere couplings (e.g. Gerber et al., 2012). A thorough understanding and accurate quantification of the UV variability effect on the middle stratosphere, from which the "top-down" theory stems, are thus necessary.

15 Solar irradiance fluctuations strongly depend on the wavelength range and their relative amplitudes tend to increase sharply with decreasing wavelengths (Lean, 2000). In the UV range, the variability over the course of the 11year solar cycle is of about 8% at 200 nm. Several observational and modeling studies have examined the impact of 11year UV variability on stratospheric ozone and temperature (e.g. Hood, 2004; Soukharev and Hood, 2006; Randel and Wu, 2007; Austin et al., 2008; Remsberg et al., 2008; Gray et al., 2009; Remsberg, 2014; Dhomse et al., 2016). These studies found a change associated with 11year solar

20 cycle in the range of 2 to 5% in ozone mixing ratio, which maximizes near 40 km. Maycock et al. (2016) recently compared the ozone 11year solar cycle signal of several different satellite records and found substantial differences. One inherent issue of the observational investigation of the 11year cycle ozone response is the fact that only three complete periods of the 11year solar cycle have been covered by satellite observations so far. Furthermore, the life span of a single satellite instrument is generally far less than one solar cycle and instrumental biases between different ozone profile data sets complicate statistical

25 analysis of decadal variations (Fioletov, 2009; Dhomse et al., 2016). In this regard, a suitable alternative for understanding better the direct effect is to examine the ozone response on Sun's rotational timescale (i.e. about 27 days). Although the irradiance fluctuations during the rotational cycle are on average smaller than during the 11year solar cycle, there are many more rotational cycles than 11year cycles, improving considerably the statistics.

A number of observational studies has been carried out to determine the effects of the solar rotational cycle on stratospheric

30 ozone, generally at low-latitudes (i.e. tropical region) based on the analysis of satellite observations (e.g. Hood, 1986; Eckman, 1986b; Keating et al., 1985; 1987; Hood et al., 1991; Fleming et al., 1995; Hood and Zhou, 1998; 1999; Fioletov, 2009; Dikty et al., 2010). These studies have shown that the sensitivity of tropical ozone to the solar rotational cycle maximizes at about 40 km (or ~3 hPa) and varies from 0.2 to 0.6% for a 1% change in solar UV radiation index, typically taken as the irradiance

at the 205 nm wavelength. It was further shown that the phase lag of the tropical stratospheric ozone response varies with the altitude. The phase lag vertical profile between the ozone response and the solar forcing was found to be negligible at about 40 km and gradually increasing (decreasing) below (above) that altitude. The phase lag was estimated to be approximately 4 days at 30 km and -2 days at 50 km (e.g. Hood, 1999; and references therein).

5   Simulations with numerical models of various complexities have been performed to understand the influence of the rotational cycle on ozone variability. One-dimensional photochemical-radiative model experiments (e.g. Hood, 1986; Eckman, 1986a; Brasseur et al., 1987) allowed identifying the importance of temperature/ozone couplings and reproducing the gross features of the observed ozone response. In particular, they found that the negative phase lag between the solar forcing and the ozone response in the upper stratosphere originated from the strong influence of the temperature feedback on ozone response through

10   the temperature dependent chemical reactions (Brasseur et al., 1987). They however noticed that including the solar induced temperature changes alone was not sufficient to adequately reproduce the observed magnitude and phase lag of the ozone response and suggested that atmospheric dynamical variability – which is not simulated in 1-D models - may also have a sizeable influence (Hood, 1986; Brasseur et al., 1987). The latter issue has later been addressed with two-dimensional models which revealed better agreement with observations (Brasseur, 1993; Fleming et al., 1995; Chen et al., 1997).

15   Using a large ensemble (nine 1year long runs) of chemistry-climate model (CCM) simulations, Rozanov et al. (2006) found that the ensemble mean ozone sensitivity to the solar rotational irradiance changes was in very good agreement with observational data. They however pointed out – despite an identical solar forcing for each experiment - a large scatter in maximum ozone sensitivities that could vary by a factor of almost 10 between the two most distant ensemble members. A large variability in ozone sensitivity was similarly found in an ensemble of three transient CCM simulations (1960-2005)

20   (Austin et al., 2007). Bossay et al. (2015) analysed satellite observations of two periods of 3 years during the declining phases of cycles 22 and 23 (i.e. 1991-1994 and 2004-2007) and found that the solar rotational signal in stratospheric ozone time series strongly varies from one year to another. These results suggest that the background dynamical state and variability of the atmosphere contribute to masking the solar rotational signal in ozone (Gruzdev et al., 2009).

In addition to the nonlinear dynamics, the intensity of the solar forcing naturally modulates the solar rotational signal in ozone.

25   When the solar rotational fluctuations are well marked with large amplitudes, notably around the maxima of 11year cycles (e.g. Rottman et al., 2004), ozone response and correlation are expected to be the largest. This has been supported by observational (e.g. Hood, 1986; Zhou et al., 2000; Fioletov, 2009; Ditky et al., 2010) as well as modeling (Kubin et al., 2011) studies which demonstrated a better identification of the ozone signal associated with enhanced rotational forcing fluctuations. This relationship has however been challenged by contradictory results. Hood and Zhou (1998) analysed MLS/UARS ozone

30   data for the 1991-1994 period and found a correlation two times stronger during the last half of the period, i.e. when the rotational forcing fluctuations are reduced. They suggested that it might have been the result of an artefact of either instrumental or geometric (local time coverage) origin that may have affected the earliest part of the MLS/UARS ozone record more than the later part. In their recent observational study which compared the declining phases of cycle 22 and cycle 23, Bossay et al.

Atmospheric
Chemistry
and Physics
Discussions

(2015) further showed that even though the amplitude of solar rotational fluctuations of the 205 nm flux was by far the largest during the first year of both periods, the correlation with tropical ozone was found to be maximum the subsequent years.

The ozone sensitivity response to the solar rotational forcing has also been suggested to vary with the intensity of the forcing. We recall that the "sensitivity" is a quantity expressed as % changes in ozone (or any other variable of interest) per % change

5   of the forcing (here specifically solar). Hence, the sensitivity is normalized by the amplitude of the forcing and may not be expected to change strongly with the amplitude of the forcing, or at least not as much as the absolute amplitude of the ozone response which directly depends on the amplitude of the forcing. Grudzev et al. (2009) used an idealized solar rotational forcing in their model (prescribed as a sinusoidal 27day oscillation) and found a significant reduction of the ozone sensitivity when applying an enhanced solar forcing amplitude (3 times the standard amplitude). Reciprocally, in the CCM experiments

10   of Kubin et al. (2011), the ozone sensitivity seemed to be enhanced during periods of weak 27 day cycles. Finally, the observational study of Bossay et al. (2015) also hints at an opposite relationship between the solar rotational irradiance fluctuations and the ozone sensitivity. Given the strong influence of the dynamical background state on the variability of estimated ozone sensitivity and the rather shortness of the considered time windows of analysis, they recognized that it was not possible to conclude to a systematic effect. All these results thus highlight the uncertainty regarding the influence of the

15   forcing intensity on ozone sensitivity and on the length of the time window required for an accurate and robust estimation of the ozone rotational signal.

In the present study, we examine the sensitivity of the tropical stratospheric ozone response to the rotational cycle by comparing satellite observations and chemistry climate model experiments to understand better the origin of the discrepancies - and sometime contradictory results - in the estimation of the ozone response to the solar rotational cycle found in previous studies.

20   In particular, we aim to (i) assess the influence of the solar cycle phase on the ozone sensitivity to the rotational cycle and (ii) quantify the time window required for a robust estimation of the ozone sensitivity. Two configurations of the LMDz-Reprobus chemistry climate model simulations are used, with specified dynamics (i.e. Chemistry Transport Model, or CTM) and in its free running mode (CCM). In the CTM configuration, temperature and wind fields calculated by the model are relaxed towards meteorological analysis; the dynamics is expected to be rather close to the reality, allowing direct comparisons with satellite

25   observations for evaluating model chemical processes and its relevance to our study. Then, an ensemble of CCM simulations is performed to examine the ozone sensitivity as a function of the solar cycle phase and the size of the analysis time window. Performing an ensemble of simulations allows us to assess better the statistical robustness of the results.

Observational datasets, and model configurations and simulations are described in section 2. Section 3 presents comparisons between satellite observations and model (CTM and CCM) simulations of the ozone response to the solar rotational cycle.

30   Section 4 focuses on CCM results to examine the influence of (i) the solar activity fluctuations and (ii) the length of the time window in the estimation of the ozone sensitivity to the solar rotational cycle. The main findings are summarized in section 5. Note that for the sake of simplicity, the first period (10/1991-09/1994) during cycle 22 will be referred thereafter as 1991-94 period and the second period (09/2004-08/2007) during cycle 23 will be referred as 2004-07 period.

2 Data and model description

2.1 The 205 nm solar flux (or F205)

The solar proxy used in regressions analyses is the UV solar irradiance at 205 nm. This wavelength is chosen because it is important for the ozone chemical budget throughout the stratosphere. The 205 nm wavelength is included in the Herzberg

5   continuum region (200-242 nm) that is positioned between two strong absorption bands: the Schumann–Runge band of molecular oxygen and the Hartley band of ozone (Brasseur and Solomon, 2005). In the Herzberg continuum, atmospheric absorption is relatively low and hence solar UV radiation penetrates deeply in the atmosphere, down to the lower stratosphere, where it photolysis molecular oxygen (O_2) to produce O_3. The 205 nm flux, called thereafter F205, has been commonly used in previous studies because it is a very good proxy for characterizing solar variability in the UV domain.

10   In our study, we use the solar spectral irradiance provided by the Naval Research Laboratory Solar Spectral Irradiance (NRLSSI) model (Lean, 2000; Wang et al., 2005). NRLSSI is an empirical model which aims to reconstruct long-term SSI over the wavelength domain 120-100,000 nm. It uses historical estimates of faculae brightening and sunspot darkening to extend in time wavelength-dependent parameterizations of SSI derived from satellite measurements and model. Shortwards of 400 nm, the SSI is derived from UARS/SOLSTICE observations (Rottman et al., 2001) through a multiple regression analysis

15   with respect to a SOLSTICE reference spectrum. The regression analysis includes a facular brightening and a sunspot darkening time-dependent term. Above 400 nm the SSI is reconstructed by adding the irradiance changes caused by the presence and the characteristics of faculae and sunspots (see Lean (2000) for details) to a quiet Sun intensity spectrum, i.e., defined by the absence of faculae and sunspots. The intensity spectrum of the quiet Sun is a composite compiled from space-based observations made by UARS/SOLSTICE (120-401 nm) and SOLSPEC/ATLAS-1 (401-874 nm) (Thuillier et al., 1998),

20   and a theoretical spectrum at longer wavelengths (Kurucz, 1991).

2.2 Microwave Limb Sounder ozone satellite observations

We use the stratospheric ozone measurements from the two Microwave Limb Sounder (MLS) instruments on-board UARS (cycle 22) and Aura (cycle 23).

MLS-UARS was launched on 12 September 1991, into a 57° inclination and a 585 km altitude orbit and was operational until

25   1994. Waters (1989; 1993) describe in detail the microwave limb-sounding technique. The ozone retrieval is based on 205 GHz radiances. The typical 1σ precision for ozone mixing ratio measurements is 0.5 ppmv at 0.46 hPa, 0.3 ppmv at 1-4.6 hPa and 0.2 ppmv at 10-46 hPa. As shown in Hood and Zhou (1998), an artificial 36day periodicity, caused by the UARS yaw manoeuvre cycle (Froidevaux et al., 1994), is seen in zonally averaged MLS-UARS data at all latitudes and increasing with height. To remove this artefact, Hood and Zhou (1998) suggested restricting zonal averaging ozone profiles to daytime

30   measurement near a single local time. They however recognized that the ratio of daytime measurements per day would be too low (around 30%), resulting in very large sampling errors and time gaps in the zonal averages.

Atmospheric
Chemistry
and Physics
Discussions

MLS-Aura was launched on 15 July 2004 into a sun-synchronous near-polar orbit around 705 km. Detailed information on the MLS-Aura instrument is given in Waters et al. (2006). In brief, MLS-Aura observes a large suite of atmospheric parameters by measuring millimeter and submillimeter-wavelength thermal emission from Earth's limb with seven radiometers covering five broad spectral regions (118, 190, 240, 640 GHz and 2.5 THz). The "standard product" of ozone is retrieved from radiance measurement near the 240 GHz. Here, we used version 4.2 of the MLS-Aura ozone product. The MLS-Aura fields of view point forward in the direction of orbital motion and vertically scan the limb in the orbit plane, resulting in a data coverage from 82°N to 82°S latitude on every orbit. MLS-Aura provides continuous daily sampling of both polar regions without temporal gaps from yaw maneuvers that occurred with MLS-UARS. The MLS-Aura limb scans are synchronized to the Aura orbit, with 240 scans per orbit at essentially fixed latitudes. This results in about 3500 scans per day, with an along-track separation between adjacent retrieved profiles of 1.5° great circle angle. The vertical resolution is about 3 km in the upper troposphere and stratosphere and about 4-6 km in the mesosphere. The 1σ precision for ozone mixing ratio measurements is about 0.1 to 0.3 from 46 hPa to 0.5 hPa.

For our study, daily stratospheric ozone profiles averaged over the tropical band [20°S,20°N] are used. Among the 1095 days of each period, 121 and 38 days of ozone data are missing for the period 1991-94 and 2004-07, respectively. For each height level of the vertical profile, the outliers of the corresponding ozone time series are removed by excluding data which take absolute values beyond 2 standard deviations of the deaseasonnalized time series. After removing outlier values, 85% (93%) of the 1095day ozone time series of the period 1991-94 (2004-07) are kept for the analysis.

2.3 The LMDz-Reprobus model

The LMDz-Reprobus model is a Chemistry-Climate Model resulting from the coupling between the extended version of the General Circulation Model LMDZ5 (Sadourny and Laval, 1984; Le Treut et al., 1994; 1998; Lott et al., 2005; Hourdin et al., 2006; 2013) and the chemistry module of the Reprobus stratospheric chemistry-transport model (Lefèvre et al., 1994; Lefèvre et al., 1998). LMDZ was developed at the Laboratoire de Météorologie Dynamique (LMD). The dynamical part of the code is based on a finite-difference formulation of the primitive equations of meteorology (Sadourny and Laval, 1984). The model uses a classical hybrid σ-P coordinate in the vertical, has 39 vertical levels and a lid-height at ~70 km. The model is integrated with a horizontal resolution of 3.75° in longitude and 1.9° in latitude. The equations are discretized on a staggered and stretched latitude-longitude Arakawa-C grid.

The Reprobus chemistry model (Jourdain et al., 2008; Marchand et al., 2012) calculates the chemical evolution of 55 atmospheric species and includes a comprehensive description of the stratospheric chemistry (Ox, NOx, HOx, ClOx, BrOx and CHOx). It uses 160 gas-phase reactions and 6 heterogeneous reactions on sulfuric acid aerosols and PSCs. Absorption cross-sections and kinetics data are based on the 2011 Jet Propulsion Laboratory (JPL) evaluation (Sander et al., 2011). In the troposphere, where the chemistry is not explicitly treated, the model is relaxed towards a monthly varying climatology (annual cycle) of O_3, CO and NOx computed by the TOMCAT chemical-transport model (Law et al., 1998; Savage et al., 2004).

Atmospheric
Chemistry
and Physics
Discussions

The solar component of the radiative scheme of LMDZ5 is based on an improved version of the two bands scheme developed by Fouquart and Bonnel (1980) and the thermal infrared part of the radiative code is taken from Morcrette et al. (1986). While this scheme is crude, note that the thermal component of the solar forcing (e.g. changes in net heating from solar changes only, keeping chemical composition unchanged) does not exhibit a dependency on wavelength as strong as photolysis component

5   of the solar forcing. Nonetheless, the use of a simple two bands radiation code tends to underestimate the temperature response when compare to other radiations models with the same solar irradiance fluctuations (CCMVal, 2010; Forster et al., 2011). The radiative scheme takes into account the radiative active species H_2O, CO_2, O_3, N_2O, CH_4, CFC-11 and CFC-12. The photolysis rates used in Reprobus are pre-calculated off-line with the Tropospheric and Ultraviolet Visible (TUV) model (Madronich and Flocke, 1999) and then tabulated in a look-up table for 101 altitudes, 7 total ozone columns and 27 solar zenith

10   angles. TUV calculates in spherical geometry the actinic flux, scattering and absorption through the atmosphere by the multi-stream discrete ordinate method of (Stamnes et al., 1988). The spectral domain extends from 116 to 850 nm. Calculations of photolysis rate are performed on a 1 nm wavelength grid, except in the regions relevant for solar cycles (rotational and 11-year solar cycles). In these spectral regions, the resolution is largely increased to accurately describe the spectral features in the solar flux or in the absorption cross-sections: the wavelength resolution increases up to 0.01 nm in the Schumann-Runge bands

15   of O_2. At this resolution, the absorption by O_2 can be considered to be treated line-by-line. Moreover, the temperature dependent polynomial coefficient determined by Minschwaner et al. (1992) is used. The temperature dependence of absorption cross-sections is taken into account using climatological temperature profiles. The albedo considered for the computation of photolysis rates is set to a globally average value of 0.3 with solar zenith angle varying from 0 to 95°. For each sunlit grid point, the actual photolysis rates used by LMDz-Reprobus are then interpolated in the table according to those parameters

20   (solar zenith angle, ozone column, altitude). Thus, the solar rotational cycle forcing is taken into account by using daily photolysis rates calculated by TUV in the photochemistry module of LMDz-Reprobus. We do not take into account the direct effect on heating rates generated by UV variations because previous modelling studies have already shown that the stratospheric ozone response to solar variations is almost entirely driven by the effects of UV changes on the photolysis rates, in particular the photolysis of molecular oxygen (Swartz et al., 2012).

25   LMDz-Reprobus is used in two configurations. The first one is the free-running model configuration (i.e. CCM) that accounts for all the interactions between chemistry, dynamics and radiation. LMDz-Reprobus is additionally used in its nudged version (i.e. CTM) where transport and dynamics are nudged towards temperatures and winds from the 6 hourly ECMWF model outputs (ERA-interim (Dee et al., 2011). As the dynamics is specified and is close to observations, the CTM configuration allows a fair comparison with MLS observations. The CTM configuration is used over the two 3year periods of MLS ozone

30   measurements, as analysed in Bossay et al. (2015). In the CCM configuration, we perform an ensemble of five simulations of 17 years each (from 1991 to 2007). As for the observations, we use the daily stratospheric ozone profiles averaged over the tropical band [20°S,20°N].

3 Ozone response to the solar rotational cycle during the declining phase of solar cycles 22 and 23

In this section, we analyse the ozone response to the solar rotational cycle over the declining phase of solar cycles 22 and 23 in the observations and the different model configurations. Note that the present modelling study partly follows on from Bossay et al. (2015) observational study. As such, few of their results are shown next to our model results for comparison.

3.1 The rotational cycle in UV irradiance

Figure 1 shows the solar UV variability represented by F205 from 1985 to 2008 with the two periods of interest highlighted in red which correspond to the declining phase of solar cycles 22 and 23. F205 is a good indicator of the NRLSSI solar forcing prescribed in CTM and CCM simulations. Thereafter, F205 is used as the UV index in the regression analysis of the solar signal in stratospheric ozone from MLS observations and model simulations.

The Fast Fourier Transform (FFT) power spectra of the two F205 declining periods time series are shown on Fig. 2 (top panel). For both periods, the high frequency spectrum is dominated by a strong peak centred around 27 days corresponding to the main solar rotational periodicity. The broadness of the peaks indicates that the solar rotational cycle is not regular and cover a rather wide frequency domain. A small secondary peak is also found at ~13.5 days which corresponds to the first harmonic of the rotational cycle and to the presence on the Sun surface of two sunspots which rotate with the same period but are separated by about 180° in longitude (e.g. Bai, 2003; Zhang et al., 2007). The time-resolved power spectral density derived from the continuous wavelet transforms (CWT, (Torrence and Compo, 1998)) of the two F205 time series are shown on Fig. 2 (bottom panels). CWT spectral analysis reveals that the solar rotational component strongly varies in time for both declining periods. Overall, the rotational component decreases over the declining solar activity periods and even can sporadically disappear for several months (e.g. late boreal summer 1993, spring 2006 and winter/spring 2006/2007). In addition, the solar rotational fluctuations are stronger during the first period than the second period (see Fig. 1 and 2). As the solar rotational forcing is stronger during the first period, one might expect the solar signal in ozone to be clearer.

3.2 Observed and modelled ozone response to the rotational cycle

We first examine potential rotational periodicities in upper stratospheric tropical ozone by carrying out a spectral analysis of daily stratospheric ozone time series averaged over the tropical band [20°S-20°N]. Figure 3 shows the normalized Lomb-Scargle periodograms (well adapted for non-continuous series, Lomb (1976); Scargle (1982)) of tropical stratospheric ozone from observations (Figs. 3a,d), CTM (Figs. 3b,e) and CCM results (Figs. 3c,f), calculated for the declining period of cycle 22 (Figs. 3a,b,c) and cycle 23 (Figs. 3d,e,f). Periodograms are shown for the 3.2 hPa (~40 km) pressure level, close to the altitude where the ozone solar signal maximizes (Hood, 1986).

The two periodograms of MLS ozone measurements (Fig. 3a and Fig. 3d) reveal no prominent peak in the range of the 20-30 days period, indicating that the solar rotational signal in ozone is weak. More prominent peaks are found at longer periods although they are not consistent between the two periods. The large peak found at the 35day period for 1991-94 corresponds

to the yaw-maneuver period of the MLS instrument as described previously (Froidevaux et al., 1994; Hood and Zhou, 1998). Similarly to observations, the periodograms of CTM results (Fig. 3b and Fig. 3e) does also not exhibit a distinctive solar rotational peak; there are some minor peaks between 20 and 30 days and their amplitudes are smaller in 2004-07 than in 1991-94.

5   In contrast, the periodogram averaged over the five CCM simulations exhibits a distinctive peak centred at 27 days for 1991-94 (Fig. 3c). This peak is less pronounced and centred at 25 days for 2004-07 (Fig. 3f), presumably because of the smaller amplitude of solar rotational fluctuations and hence model forcing in 2004-07 (see Fig. 2). However, the 2σ standard deviation (i.e. spread of the ensemble simulations) associated with these peaks is very large, indicating the presence of a strong high frequency (periods < 50 days) natural variability in ozone in this region. This explains why solar rotational signal can be hardly

10   detectable in the observations, as well as in a single ensemble member. The absence of a distinctive rotational signal in MLS data and CTM 3year time series suggests the presence of strong and rather random ozone variability of non-solar origin which makes the ozone rotational signal very difficult to detect and estimate.

We further examine the relationship between stratospheric ozone and solar rotational cycle by performing cross-spectrum analysis between stratospheric ozone and F205. Despite the weak magnitude of the ozone rotational signal, cross-spectrum

15   analysis should help identifying coherent variability modes between the solar forcing and tropical ozone. Figure 4 presents the vertical profile of the magnitude-squared coherence (hereinafter referred as coherence) between F205 and tropical stratospheric ozone from MLS observations (a and d), CTM model results (b and e) and CCM model results (c and f).

A strong and statistically significant coherence is found for MLS-UARS (1991-94) between 20 and 28 days and between about 10 and 1 hPa with a maximum of about 0.7 at the 22day period around 6 hPa. In contrast, the coherence for MLS-Aura (2004-

20   07) is generally weaker with only a small patch of significant coherence at the 90% confidence level. The coherence fields from the CTM results resemble those of the observations and reproduce the main features during the two periods. The main difference between observed and CTM signals is that the coherence patch extends farther to lower levels in the CTM (down to 15 hPa) and covers longer periods (20 to 33 days at ~10 hPa). For the 1991-94 period, the CTM results also overestimate the coherence around 13.5 days compared to observations.

25   The general features in the coherence fields from CCM results are also consistent with those of the observations. However, the area of statistical significant coherence around the 27day period is wider in the CCM results. In addition, the coherence patch does not extend as low as the CTM results. The differences observed between the MLS coherence fields of the two periods are also reasonably well reproduced in the CCM coherence results. As for the CTM fields in 1991-94, CCM results reveal a secondary area of significant signal centred at about 13.5day period and extends almost throughout the stratosphere. For 2004-

30   07, there is no significant signal around 13-14 days in all the coherence fields. This is consistent with the UV forcing (Fig. 2) exhibiting a stronger 13.5day period component in 1991-94.

To further test the robustness of the coherence signal, we perform an additional CCM simulation where the solar forcing is kept constant by using fixed (i.e. climatological) photolysis rates during the model simulation. The total absence of significant coherence found in this simulation (not shown) confirms that the coherence found between F205 and stratospheric ozone is

Atmospheric
Chemistry
and Physics
Discussions

not fortuitous and primarily originates from photolysis processes. We can also note that the reduced coherence for 2004-07 may be expected because the solar rotational fluctuations are smaller during that period compared to 1991-94 (Fig. 2). To summarize these first steps in our analysis, we find that, despite the weak magnitude of the signal, the upper stratosphere tropical ozone concentration fluctuates coherently with UV variability at solar rotational timescales.

5   To focus on periodicities relevant to the solar rotational cycle (13.5 and 27 days), all the time series are now filtered using the digital filter that has been commonly used in previous solar rotational studies (e.g; Hood, 1986; Chandra, 1986; Keating et al., 1987; Hood and Zhou, 1998 and Zhou et al., 2000). The filtering procedure consists of smoothing data with a 7day running mean which removes short-term fluctuations. Linear trend and mean value are also removed from these smoothed time series. Finally, a 35day running mean is subtracted from the data, removing long-term fluctuations (e.g. seasonal, semi-annual, annual

10   and QBO variations). The overall procedure is more or less equivalent to a 7-35 days band-pass filter in the frequency domain. The vertical extent and temporal evolution of the tropical ozone response to the solar rotational cycle are examined by calculating the cross-correlations between filtered F205 and ozone in observations and model results. Results are shown in Fig. 5. For 1991-94, the observations exhibit a cross-correlation peak at 0.28 on the 4.6 hPa level with no time lag (Fig. 5a). This maximum value is close to the maximum of 0.35 found by Hood and Zhou (1998) on the same pressure level. Furthermore,

15   the overall variation of the time lag with altitude shown in Fig. 5 is similar to that found in previous studies (Hood, 1986; Brasseur et al., 1987; Brasseur, 1993; Hood and Zhou, 1998) with a negative lag above 3-4 hPa (ozone "leading" the solar flux) and a positive lag below (ozone lagging the solar flux). As mentioned in the introduction, the negative lag in the upper stratosphere result of the influence of the temperature feedback on the ozone response through the temperature dependent chemical reactions. For 2004-07, the cross-correlation pattern (Fig. 5d) is more distorted and weaker than for 1991-94 (Fig.

20   5a). The cross-correlation maximum (0.2) is smaller than for 1991-94 and is found at 10 hPa with a time lag of +5 days (ozone lagging solar flux).

Although the cross-correlation fields for the CTM and CCM simulations appear smoother and with larger statistically significant (shaded) areas than for the MLS data, most of the general features present in the MLS cross-section fields appear consistently reproduced by the simulations in the two model configurations. Seizing differences between the CTM and the

25   observations are found in 1991-94 though. The high correlation area (with a maximum of 0.4 at 7 hPa and a positive time lag of 3 days) expanding throughout the middle stratosphere (between 30 and 10 hPa) in the CTM (Fig. 5b) is not detected in observations (Fig. 5a). Overall, the main area of significant correlation appears also lifted upward in the observations (Fig. 5a) compared to the CTM (Fig. 5b). The absence of correlation signal in the middle and lower stratosphere in the observations is consistent with the large noise present in the ozone dataset at these altitudes (not shown). In contrast, the results for the period

30   2004-07 reveal a particular good agreement throughout stratosphere between the observations (Fig. 5d) and the CTM (Fig. 5e), where the maximum is found at the same altitude (10 hPa), time lag (+4 days) and with the same amplitude (0.2). CCM results show a maximum of correlation also at 10 hPa and at the same time lag but with a higher value (0.3). In addition to the area of statistical significance which increases when examining CCM results, we notice a strong reduction of the difference in the response between both periods. This suggests that averaging over the five ensemble members allows to reduce the effect

Atmospheric
Chemistry
and Physics
Discussions

Open Access

of the non-solar random variability in the signal estimation and hence to identify more robustly the solar signal. Nevertheless, for 2004-07, we note a weaker correlation and a reduced downward propagation of its extension which is likely due to a weaker rotational UV forcing compared to 1991-94 (Figs. 1 and 2).

In addition to correlation analysis, ozone response to solar UV flux changes can also be measured in terms of sensitivity, i.e.
5   percentage change in ozone per 1% change in solar UV. Considering ozone sensitivity instead of ozone absolute change allows in principle to analyse an ozone signal that does not depend on the magnitude of the solar rotational forcing, assuming implicitly that the relationship between the solar forcing index (F205) and the ozone response is linear. We derive the ozone sensitivity on different pressure levels by linear regression of the filtered ozone time series on one independent variable, F205. Results are shown on Fig. 6.

10   For the 1991-94 period, the observational (MLS-UARS) sensitivity peaks at 0.4 (0.4% of ozone change for 1% change in F205) near 4-5 hPa (35 km), consistent with the results of Hood and Zhou (1998) (Fig. 6a). For the 2004-07 period, the shape of the observational (MLS-Aura) sensitivity profile is distorted and the sensitivity peaks at only 0.2 around 5 hPa (Fig. 6d); it is consistent with a peak value of 0.15 derived at the same level shown in Dikty et al. (2010) for a similar period (2006-07) but with a different instrument (SCIAMACHY). In the middle stratosphere, the sensitivity profile calculated from the CTM
15   results for the period 1991-94 (Fig. 6b) is consistent with the MLS sensitivity profile (Fig. 6a); the CTM sensitivity profile peaks at 4-5 hPa with a value slightly lower (0.3) than that derived from the MLS observations. Discrepancies between CTM and observational sensitivities are more pronounced in the upper stratosphere. In the CTM, above the peak, the sensitivity suddenly drops around 3 hPa to values close to 0 (Fig. 6b), while in the observation the sensitivity gradually decreases from 3-4 hPa to the stratopause region (around 1hPa) (Fig. 6a). Below 10 hPa, we also note that the sensitivity profile errors are
20   larger in the observations than in the CTM. This is consistent with the absence of solar-ozone correlation signal at these altitudes in the observations (Fig.5a) and, inversely, the clear solar-ozone correlation signal in the CTM (Fig. 5b). For 2004-07, the CTM sensitivity profile appears to be highly consistent with observations throughout the stratosphere, in accordance with the previous coherence and correlation analyses (Figs. 4 and 5).

We now analyse the CCM ensemble results. The ensemble mean ozone sensitivity profiles for the two periods are similar with
25   positive sensitivity from 15 hPa to the stratopause and a maximum sensitivity of 0.4 at ~3 hPa (Figs. 6c and f). This maximum tropical sensitivity value and its altitude level is in good agreement with previous CCM estimates (e.g. Rozanov et al., 2006; Austin et al., 2007; Gruzdev et al., 2009; Kubin et al., 2011). The ensemble spreads (i.e. 2σ standard deviation calculated over the five CCM simulations for each 3year period, dashed line) are of the same order for both periods (Figs. 6c and f). They are also very large, indicating important variations from one ensemble member to another, which are most likely due to differences
30   in dynamical variability. Similar conclusions have been reached in previous CCM studies (e.g. Rozanov et al., 2006; Austin et al., 2007). This may partly explain the strong differences in ozone sensitivity found between the two periods in the observations and the CTM simulation. In a sense, each 3year observed period can be viewed as a single realization of an ensemble.

Atmospheric
Chemistry
and Physics
Discussions

Overall, our results demonstrate that the LMDz-REPROBUS model produces an ozone response to the solar rotational cycle that is consistent with observations, especially when the dynamical variability is accounted for in the analysis. The results of our ensemble of transient CCM simulations further support the importance of atmospheric internal variability in modulating or masking the solar signal in ozone at solar rotational time scales. In the following, we exploit the ensemble simulation to

5 examine thoroughly the temporal variability of the ozone sensitivity to the rotational cycle.

4 Temporal variability of the ozone response sensitivity

4.1 Does ozone sensitivity to the rotational cycle depend on the amplitude of the solar fluctuations?

Results from CCM studies of Gruzdev et al. (2009) and Kubin et al. (2011) suggested that ozone sensitivity seems to decrease with increasing amplitude of the rotational cycle. Given that the amplitude of the rotational cycle increases with increasing

10 solar activity, one may thus expect minimum (maximum) sensitivity during 11year solar maximum (minimum) phases. Next, we test this hypothesis by dividing 15 years (1991-2005) of the CCM simulations into five 3year windows corresponding to the four different phases of the 11year solar cycle (*i.e.* maximum, minimum, descending, ascending phases). These time windows are highlighted with different colours in the insert panel of Fig. 7a. Figures 7b-f show, for each 3year time window, the ensemble mean sensitivity profiles and the associated 2σ ensemble spread. The ensemble mean for a specific 3year window

15 is calculated by first computing the ozone sensitivity over this specific 3year interval for each of the five ensemble members and then averaging theses five sensitivities; we define the ensemble spread as the ensemble 2σ standard deviation. Note that, in total, 15 years of model data are taken into account for the calculation of the ensemble mean sensitivity.

Whatever the solar cycle phase considered (Fig. 7a), all the mean sensitivity profiles have similar shapes with a maximum at around 3 hPa, consistent with observed and modelled sensitivity profiles during solar declining phase (Fig. 6). The most

20 pronounced difference is the maximum sensitivity which varies between 0.3 (green) and 0.5 (red). Overall, the ensemble mean sensitivity profiles appear to vary little from a 3year window to another. Thus, the model ensemble mean ozone sensitivity seems to be rather independent of the level of solar activity (Fig. 7a), at least when 15 years of model data are considered in total. In comparison, the model ensemble spread is clearly more sensitive to the 11year solar cycle phase than the ensemble mean. The ensemble spread is found to be generally smaller during high solar activity periods. It is not surprising. The

25 estimation of the ozone sensitivity is expected to be less affected by the noise and more robust when the solar rotational fluctuations are stronger: the amplitude of the ozone response is much greater, improving the signal-to-noise ratio. We also notice that the ensemble spread is smaller during the maximum phase of cycle 22 (black) than that of cycle 23 (green). It is consistent with the results of Fioletov (2009) observational study that also shows a stronger rotational periodicity in the upper stratosphere tropical ozone during the maximum phase of the solar cycle 22 than the maximum phase of the cycle 23.

30 Although the rotational cycle amplitude varies with the phase of the 11year solar cycle, the relationship is not systematic as revealed by the wavelet analysis of Fig. 2. In the following, the ensemble mean ozone sensitivity and its spread are examined as a function of the amplitude of the solar rotational cycle fluctuations using sliding time windows. The analysis focuses on

the 3 hPa level where the maximum sensitivity is found (Fig. 7). Figure 8 compares the temporal evolution (from 01/01/1991 to 31/12/2005) of the variance of the filtered F205 time series (Fig. 8b) with the ensemble mean (Fig. 8c) and variance (Fig. 8d) of the ozone sensitivity derived from the five CCM simulations. Each point of the time series is obtained by first calculating the ozone sensitivity for each ensemble member over a 1year time window and then computing the ensemble mean and its

5   variance over the five simulations. The time window is then shifted by 1 month and the same procedure is repeated. This gives a total of 168 1year time slices (14 years x 12 months).

The mean ozone sensitivity time series (Fig. 8c) on 1year time window strongly fluctuates from 0 to 0.6 around an average value of ~0.4, consistent with the value of the ensemble mean sensitivity profiles at 3 hPa (Fig. 7). These fluctuations increase during the minimum phase of the solar cycle in 1995-1998, indicating a larger uncertainty in the estimation of ozone sensitivity

10   during low solar activity periods. This is further supported by the overall anti-correlation which is found between the F205 index variance (Fig. 8b) and the ozone sensitivity variance (Fig. 8d). Hence, the accuracy of the ozone sensitivity estimate to solar rotational cycle is degraded when solar rotational fluctuations are small, and reciprocally. Finally, note that the low-frequency (i.e. decadal scales) variability of the ensemble mean ozone sensitivity (Fig. 8c) appears also to be anti-correlated with the F205 index variance (Fig. 8b). In the following, we test further the robustness of the relationships found here which

15   link the solar rotational variability to the ensemble mean and spread of ozone sensitivity

Figure 9 shows the regression analysis of the ensemble mean (Fig. 9a) and spread (Fig. 9b) of ozone sensitivity (i.e. dependent variables) on the solar rotational variance (i.e. explanatory variable). We assess the statistical significance of the regression slope using a block bootstrapping technique to account for the autocorrelation in the residuals that can lead to an underestimation of the standard error (Mudelsee, 2014). The bootstrap procedure is carried out as follows. The original

20   residuals are first obtained by subtracting the original fitted model (i.e. derived from the linear regression) to the dependent variable. The original residual time series is then segregated into moving blocks of length L (see e.g. schematic p74 in Mudelsee (2014)) that are randomly resampled to reconstruct a synthetic residual time series of the same size as the original one. Adding this synthetic residual time series to the original fitted model allows creating a new synthetic time series (so-called bootstrap sample) to which the linear regression is applied to derive a synthetic slope value. For each value of L, this procedure is

25   repeated 10,000 times in order to construct a distribution of synthetic slopes (Poulain et al., 2016). Finally, we estimate, from this distribution, the likelihood (p-$value$) for the slope to be greater than - or equal to - 0 (i.e. null hypothesis). Note that since L is not known a priori, the calculation is repeated for $L=1, 2, 3, ..., 10,..., 20$, etc. and the largest p-$value$ is retained.

Figure 9a reveals no significant negative trend between the mean ozone sensitivity and the F205 variance. Although the linear regression hints at increasing mean ozone sensitivity for decreasing F205 variance, the likelihood for the slope to be positive

30   or equal to zero cannot be excluded statistically ($p > 0.10$). In addition, a non-significant correlation coefficient of -0.19 between the mean ozone sensitivity and the F205 variance is found. This is not the case for the spread of ozone sensitivity, which significantly increases with decreasing high-frequency (short-term) F205 variability (Fig. 9b). This trend further intensifies for the lowest F205 variance values (black and purple dots), corresponding to the phase of the solar cycle with the lowest activity (see insert panel on Fig. 9b). This quantitative analysis hence confirms that the accuracy of the ozone sensitivity

13

Atmospheric
Chemistry
and Physics
Discussions

estimation increases when the F205 fluctuations are large. We similarly tested the dependence of the mean ozone sensitivity and its spread to the absolute value of F205 (shown in the insert of Fig. 8a), an indicator of solar activity. Results are not shown here for brevity. Although we obtain results consistent with those based on the F205 variance (which is expected given the close connection between solar cycle activity and solar rotational fluctuations), the statistical significance is found to be less

5 pronounced, suggesting a closer link with the amplitude of the fluctuations of the rotational solar cycle rather than the absolute values of F205.

4.2 Influence of the size of the time window analysis

Finally, the robustness of the estimated ozone sensitivity is examined with respect to the size of the time window. The procedure is as follows. For each ensemble simulation (of maximum size t_{max}=15 years), a time window of a given size, say

10 Δt, (Δt is comprised between 1 and 15 years) sliding by a 1year step is used to resample the ozone 15year time series and create $n_{ensemble, windows}(\Delta t)$ $(= t_{max}-\Delta t+1)$ shorter time series of size Δt. Given that the ensemble contains five simulations, the total number of samples for a given Δt is thus $n_{windows}$=5 x $n_{ensemble, windows}(\Delta t)$ (i.e. 75, 45, 5 samples for 1, 7, 15year time windows, respectively). For each time window size, the ozone sensitivity to F205 is estimated per individual sample. Finally, the mean ozone sensitivity and its spread are derived by calculating the average and the standard deviation over all samples.

15 Figure 10a shows the ozone sensitivity profiles when a 1year time window is considered. In agreement with the previous ensemble mean ozone sensitivity profiles calculated for 3year time windows and at different solar cycle phases (Figs 6 and 7), a maximum mean sensitivity of 0.4 is found near 3 hPa. The ozone sensitivity spread (dashed envelop) is larger though and even expands towards negative values, demonstrating that a 1year window is not at all long enough to estimate robustly the ozone sensitivity. Figure 10b focuses on the 3 hPa pressure level, where the sensitivity peaks, and reveals that, as expected,

20 the longer the time window is, the smaller the spread is. Figure 10c shows the coefficient of variation of the ozone sensitivity (1σ standard deviation normalized by the mean and expressed in percent) as a function of the size of the time window. It is found that a minimum time window size of 3 years or 10 years is required for the standard deviation to drop under 50% or 20%, respectively, of the mean sensitivity (i.e. ~0.4). These uncertainty ranges additionally depend on the amplitude of the solar rotational variations and hence the phase of the 11year solar cycle; we find that during solar maximum of cycle 23,

25 minimum of cycle 22, a minimum time window size of 2 or 5 years, respectively, is required for the standard deviation to drop under 50%. These results demonstrate that long time series are required for an accurate estimation of the ozone sensitivity to solar rotational fluctuations in observations. It is very likely that some, if not most, of the discrepancies between estimates of the ozone sensitivity found in previous studies originate from differences in the periods and lengths of the considered time windows.

Atmospheric
Chemistry
and Physics
Discussions

Open Access

5 Summary and concluding remarks

In this paper, we examined the tropical stratosphere ozone response to the solar rotational cycle in satellite observations and simulations of the chemistry-climate model LMDz-Reprobus. We first focused our analysis on the case study of two 3year periods associated with the declining phases of solar cycles 22 and 23. The solar rotational fluctuations are stronger during the first period than the second period. We found that, although the solar rotational signature in the UV forcing is reasonably well marked during both periods, the amplitude of ozone variations expected at the corresponding timescales (i.e. ~27 days), in observational records and individual model realizations, does not significantly differ from the noise. Nonetheless, UV and ozone fluctuations show a statistical significant coherence in the middle and upper tropical stratosphere (above ~30 km, or 10 hPa) at the solar rotational timescales. These results hence suggest that ozone significantly responds to the solar rotational variations but the signal is partly masked by other sources of ozone variability at these timescales, most likely of dynamical origin. Applying the same spectral analysis to the average of CCM ensemble simulations allows reducing the 'masking' effect by random dynamical variability, so that the rotational signal in ozone can be more easily identified and estimated.

Lag correlations and linear regressions have then been used to characterize the vertical profile of the ozone response to the solar rotational cycle in the observations and the model during the same periods. Although these results are consistent with estimates of previous studies (Hood, 1986; Brasseur et al., 1987; Brasseur, 1993; Hood and Zhou, 1998) and a reasonable agreement is found between the MLS observations and the CTM experiments, significant differences are found between the two periods. This may be attributed to differences in solar UV forcing or in dynamical variability between the two periods. Analysis of the CCM ensemble simulations suggest that the differences mostly originate from the dynamical variability. The large spread in the ensemble mean sensitivity profile calculated for 3year intervals reflects the 'masking' effect of non-solar dynamical variability in the estimation of the solar rotational signal in ozone and may certainly explain some inconsistencies found in previous studies.

Given the good representation of the ozone response to the solar rotational cycle calculated by our model in the CTM configuration, we take advantage of the ensemble of five CCM simulations to test whether the ozone sensitivity depends on the phase of the 11year solar cycle. Considering an ensemble of simulations allows in particular to reduce the masking effect induced by the dynamical random variability. Our results suggest that the level of solar activity does not have an impact on the expected value (i.e. ensemble mean) of the ozone sensitivity. However, the ensemble spread decreases during high solar activity periods, making the ozone sensitivity retrieval easier and more robust, e.g., during the maximum phase of the 11year solar cycle.

The ensemble mean ozone sensitivity and its spread have been additionally examined as a function of the amplitude of (i) the solar rotational cycle fluctuations (shown) and (ii) the phase of the 11year solar cycle (not shown). Here again, no robust dependence of the ensemble mean ozone sensitivity against each of the two variable is found when the results of the five 15year simulations are averaged. Although the results hint at a slightly negative trend, i.e. increasing ensemble mean ozone sensitivity for decreasing rotational fluctuations (or 11year solar cycle activity), neither the slopes nor the correlation

coefficients are statistically significant. Hence, our results could not confirm previous findings of Grudzev et al. (2009) or Kubin et al. (2011) who, using model experiments, suggested an increased ozone sensitivity with decreasing solar rotational fluctuations. Nevertheless, it must be noted that the conclusions of Gruzdev et al. were reached by carrying out experiments with a solar rotational forcing that had an amplitude 3 times larger than a realistic one. Further model experiments, considering

5 for instance longer simulations and/or stronger forcing, would help to address this issue more thoroughly.

In contrast with the ensemble mean ozone sensitivity, as expected, the ensemble spread ozone sensitivity shows a clear increase with decreasing solar rotational cycle fluctuations. The negative trend further intensifies during the period with very low solar rotational fluctuations, corresponding here to the period of minimum solar activity between the end of the solar cycle 22 and the beginning of the solar cycle 23 (i.e. 1994-1997). These findings are consistent with the results of Fioletov (2009) who

10 showed a noticeable difference in the estimate of the ozone sensitivity profile in 1994-1998 by comparison with other periods. Hence, when the solar rotational fluctuations are small, the 'masking' effect of dynamical variability becomes more prominent and makes the estimate of the ozone sensitivity less accurate.

Finally, we demonstrate that, while the mean ozone sensitivity (e.g. ~0.4 at 3 hPa) is more or less independent of the size of the time window (tested from 1 to 15 years) when the results of the five 15year simulations are analysed and averaged, the

15 accuracy of its estimate improves dramatically with increasing size of the time window. We found that, on average, a minimum time window size of 3 years (corresponding to ~40 solar rotational cycles) is needed for the 2σ uncertainty to drop below 100%. More concretely, this means that if the ozone sensitivity to solar rotational fluctuations is derived over only three successive years of observations (or of a single model realization), there is a 95% likelihood for the estimate to take any value in the range [0-0.8] at 3 hPa. The error in the sensitivity estimation also depends on the amplitude of the solar rotational

20 fluctuations and is thus linked to the solar activity. For a constant uncertainty threshold, the higher the solar activity is, the shorter the required time window length is. We finally find that a minimum of 10 years of data is required for the 1σ uncertainty in the ozone sensitivity estimate to drop under 20%.

Overall, it is likely that the discrepancies in the estimated value of ozone sensitivity found in previous studies originate from differences in the length of time windows that were used for analysis and in the level of solar activity associated with these

25 periods. Both parameters significantly influence the accuracy of solar rotational signal estimates. In this regard, it is likely that similar issues have also affected the accuracy in the estimation of ozone response to the 11year solar signal. The estimation is expected to be even more difficult because observational time series cover a very limited number of 11-year cycles and there are other well-known sources of decadal variability in the atmosphere and climate system. Maycock et al. (2016) recently found very large discrepancies in the estimation of the ozone response the 11year cycle using various satellite datasets which

30 cover different time periods of different length.

Atmospheric
Chemistry
and Physics
Discussions

References

Austin, J., Hood, L., and Soukharev, B.: Solar cycle variations of stratospheric ozone and temperature in simulations of a
10   coupled chemistry-climate model, *Atmos. Chem. Phys.*, 7(6), 1693–1706, 2007.

Austin, J., Tourpali, K., Rozanov, E., Akiyoshi, H., Bekki, S., Bodeker, G., Brühl, C., Butchart, N., Chipperfield, M., Deushi, M., Fomichev, V. I., Giorgetta, M. A., Gray, L., Kodera, K., Lott, F., Manzini, E., Marsh, D., Matthes, K., Nagashima, T., Shibata, K., Stolarski, R. S., Struthers, H., and Tian, W.: Coupled chemistry climate model simulations of the solar cycle in ozone and temperature, *J. Geophys. Res.*, 113, D11306, doi:10.1029/2007JD009391, 2008.

15   Bai, T.: Hot spots for solar flares persisting for decades: longitude distributions of flares of cycles 19-23, *Astrophys. J.*, 585(2), 1114, 2003.

Bossay, S., Bekki, S., Marchand, M., Poulain, V., and Toumi, R.: Sensitivity of tropical stratospheric ozone to rotational UV variations during the declining phases of solar cycles 22 and 23, *J. Atmos. Solar-Terr. Phys.*, 130-131, 10.1016/j.jastp.2015.05.014, 2015

20   Brasseur, G., De Rudder, A., Keating, G., and Pitts, M.: Response of middle atmosphere to short-term solar ultraviolet variations: 2. theory, *J. Geophys. Res.*, 92(D1), 903–914, 1987.

Brasseur, G.: The response of the middle atmosphere to long-term and short-term solar variability: A two-dimensional model, *J. Geophys. Res.*, 98(D12), 23,079–23,090, 1993.

Brasseur, G. and Solomon, S.: *Aeronomy of the middle atmosphere: chemistry and physics of the stratosphere and mesosphere*,
25   vol. 32, Springer Science & Business Media, 2005

CCMVal, S., SPARC report on the evaluation of chemistry–climate models. V. Eyring, T.G. Shepherd, and D. W. Waugh, eds., SPARC rep. 5, wcrp-132, Tech. rep., WMO/TD-1526, 434 pp.[Available online at www. sparc-climate. org/publications/sparc-reports/.], 2010

Chen, L., London, J., and Brasseur, G.: Middle atmosphere ozone and temperature responses to solar irradiance variations over
30   27day periods, *J. Geophys. Res.*, 102, 29957–29979, 1997.

Dee, D.P., Uppala, S.M., Simmons, A.J., Berrisford, P., Poli, P., Kobayashi, S., Andrae, U., Balmaseda, M. A., Balsamo, G., Bauer, P., Bechtold, P., Beljaars, A. C. M., van de Berg, L., Bidlot, J., Bormann, N., Delsol, C., Dragani, R., Fuentes, M., Geer, A. J., Haimberger, L., Healy, S. B., Hersbach, H., Hólm, E. V., Isaksen, L., Kållberg, P., Köhler, M., Matricardi, M., McNally, A. P., Monge-Sanz, B. M., Morcrette, J.-J., Park, B.-K., Peubey, C., de Rosnay, P., Tavolato, C., Thépaut, J.-N., and

5   Vitart, F.: The ERA-Interim reanalysis: configuration and performance of the data assimilation system, *Q. J. Roy. Meteor. Soc.*, 137, 553–597, 2011.

Dhomse, S., Chipperfield, M. P., Damadeo, R. P., Zawodny, J. M., Ball, W., Feng, W., Hossaini, R., Mann, G. W., and Haigh, J. D.: On the ambiguous nature of the 11-year solar cycle signal profile in stratospheric ozone, *Geophys. Res. Lett.*, 43, 7241–7249, doi:10.1002/2016GL069958, 2016.

10   Dikty, S., Weber, M., von Savigny, C., Sonkaew, T., Rozanov, A., and Burrows, J.P.: Modulations of the 27-day solar rotation signal in stratospheric ozone from scanning imaging absorption spectrometer for atmospheric cartography (SCIAMACHY) (2003–2008), *J. Geophys. Res.*, 115(D1), 2010

Eckman, R. S.: Response of ozone to short-term variations in the solar ultraviolet radiance. 1. A theoretical model, *J. Geophys. Res.*, 91, 6695–6704, 1986a.

15   Eckman, R. S.: Response of ozone to short-term variations in the solar ultraviolet irradiance: 2. observations and interpretation, *J. Geophys. Res.*, 91(D6), 6705–6721, 1986b.

Fioletov, V.: Estimating the 27-day and 11-year solar cycle variations in tropical upper stratospheric ozone, *J. Geophys. Res.*, 114(D2), 2009.

Fleming, E. L., Chandra, S., Jackman, C.H., Considine, D.B., and Douglass, A.R.: The middle atmospheric response to short

20   and long term solar UV variations: Analysis of observations and 2d model results, *J. Atmos. Solar-Terr. Phys.*, 57(4), 333–365, 1995.

Forster, P. M., Fomichev, V. I., Rozanov, E., Cagnazzo, C., Jonsson, A. I., Langematz, U., Fomin, B., Iacono, M. J., Mayer, B., Mlawer, E., Myhre, G., Portmann, R. W., Akiyoshi, H., Falaleeva, V., Gillett, N., Karpechko, A., Li, J., Lemennais, P., Morgenstern, O., Oberländer, S., Sigmond, M., and Shibata, K.: Evaluation of radiation scheme performance within chemistry

25   climate models, *J. Geophys. Res.-Atmos.*, 116, D10302, doi:10.1029/2010JD015361, 2011.

Fouquart, Y. and Bonnel, B.: Computations of solar heating of the earth's atmosphere- a new parameterization, *Beitraege zur Physik der Atmosphaere*, 53, 35–62, 1980.

Fröhlich, C. and Lean, J.: Solar Radiative Output and its Variability: Evidence and Mechanisms. *Astron. and Astrophys. Rev.*, 12, pp. 273-320, 2004, doi: 10.1007/s00159-004-0024-1, 2004.

30   Froidevaux, L., Waters, J.W., Read, W.G., Elson, L.S., Flower, D.A., and Jarnot, R.F.: Global ozone observations from the UARS MLS: An overview of zonal-mean results, *J. Atmos. Sci.*, 51(20), 2846–2866, 1994.

Gerber, E. P., Butler, A., Calvo, N., Charlton-Perez, A., Giorgetta, M., Manzini, E., Perlwitz, J., Polvani, L. M., Sassi, F., Scaife, A. A., Shaw, T. A., Son, S.-W., and Watanabe, S.: Assessing and understanding the impact of stratospheric dynamics and variability on the earth system, *B. Am. Meteorol. Soc.*, 93, 845–859, doi: 10.1175/bAms-d-11-00145.1, 2012.

Gray, L. J., Rumbold, S.T., and Shine, K.P.: Stratospheric temperature and radiative forcing response to 11-year solar cycle changes in irradiance and ozone, *J. Atmos. Sci.* 66, 2402–2417, 2009.

Gray, L. J., Beer, J., Geller, M., Haigh, J. D., Lockwood, M., Matthes, K., Cubasch, U., Fleitmann, D., Harrison, G., Hood, L., Luterbacher, J., Meehl, G. A., Shindell, D., van Geel, B., and White, W.: Solar influence on climate, *Rev. Geophys.*, 48,
5 RG4001, doi:10.1029/2009RG000282, 2010.

Gruzdev, A., Schmidt, H., and Brasseur, G.: The effect of the solar rotational irradiance variation on the middle and upper atmosphere calculated by a three-dimensional chemistry-climate model, *Atmos. Chem. Phys.*, 9(2), 595–614, 2009.

Hood, L.L.,:Coupled stratospheric ozone and temperature responses to short-term changes in solar ultraviolet flux: An analysis of NIMBUS 7 SBUV and SAMS data, *J. Geophys. Res.*, 91(D4), 5264–5276, 1986.

10 Hood, L. L., Huang, Z., and Bougher, S. W.: Mesospheric effects of solar ultraviolet variations: Further analysis of SME IR ozone and Nimbus 7 SAMS temperature data, *J. Geophys. Res.*, 96, 12989–13002, 1991.

Hood, L., and Zhou, S.: Stratospheric effects of 27-day solar ultraviolet variations: An analysis of UARS MLS ozone and temperature data, *J. Geophys. Res.*, 103(D3), 3629–3638, 1998.

Hood, L. L. and Zhou, S.: Stratospheric effect of 27-day solar ultraviolet variations: The column ozone response and
15 comparison of solar cycles 21 and 22, *J. Geophys. Res.*, 104, 26473–26479, 1999.

Hood, L.L.: Effects of short-term solar UV variability on the stratosphere, *J. Atmos. Solar-Terr. Phys.*, 61, 45– 51, 1999.

Hood, L. L.: Effects of solar UV variability on the stratosphere, *Solar variability and its effects on climate*, pp. 283–303, 2004.

Hourdin, F., Musat, I., Bony, S., Braconnot, P., Codron, F., Dufresne, J.L., Fairhead, L., Filiberti, M.A., Friedlingstein, P., Grandpeix, J. Y., Krinner, G., Levan, P., Li, Z. X., and Lott, F.: The LMDZ4 general circulation model: Climate performance
20 and sensitivity to parametrized physics with emphasis on tropical convection, *Clim. Dynam.*, 27, 787–813, 2006.

Hourdin, F., Foujols, M.-A., Codron, F., Guemas, V., Dufresne, J.-L., Bony, S., Denvil, S., Guez, L., Lott, F., Ghattas, J., Braconnot, P., Marti, O., Meurdesoif, Y., and Bopp, L.: Impact of the LMDZ atmospheric grid configuration on the climate and sensitivity of the IPSL-CM5A coupled model, *Clim. Dyn.*, 40: 2167. doi:10.1007/s00382-012-1411-3, 2013.

Jourdain, L., Bekki, S., Lott, F., and Lefèvre, F.: The coupled chemistry-climate model LMDz-Reprobus: description and
25 evaluation of a transient simulation of the period 1980–1999, *Ann. Geophys.*, 26(6), 1391–1413, 2008.

Keating, G. M., Brasseur, G. P., Nicholson III, J. Y., and De Rudder, A.: Detection of the response of ozone in the middle atmosphere to short-term solar ultraviolet variations, *Geophys. Res. Lett.*, 12, 449–452, 1985.

Keating, G., Pitts, M., Brasseur, G.P., and De Rudder, A.: Response of middle atmosphere to shortterm solar ultraviolet variations: 1. observations, *J. Geophys. Res.*, 92(D1), 889–902, 1987.

30 Kodera, K. and Kuroda, Y.: Dynamical response to the solar cycle. *J. Geophys. Res.* 107, 4749 2002.

Kopp, G., and Lean, J.L.: A new, lower value of total solar irradiance: Evidence and climate significance, *Geophys. Res. Lett*, 38(1), 2011.

Kubin, A., Langematz, U., and Brühl, C.: Chemistry climate model simulations of the effect of the 27-day solar rotational cycle on ozone, *J. Geophys. Res.*, 116, D15301, doi:10.1029/2011JD015665, 2011.

Kurucz, R. L.: New Opacity Calculations, in *NATO Advanced Science Institutes* (ASI) *Series C*, vol. 341, edited by L. Crivellari, I. Hubeny, and D. G. Hummer, p. 441, 1991.

Law, K., Plantevin, P., Shallcross, D., Rogers, H., Pyle, J., Grouhel, C., Thouret, V., and Marenco, A.: Evaluation of modeled O_3 using measurement of ozone by airbus in-service aircraft (MOZAIC) data, *J. Geophys. Res.*, 103(D19), 25,721–25,737,

5   1998.

Le Treut, H., Li, Z., and Forichon, M.: Sensitivity study of the LMD GCM to greenhouse forcing associated with two different cloud water parametrizations, *J. Clim.*, 7, 1827–1841, 1994.

Le Treut, H., Forichon, M., Boucher, O., and Li, Z.-X.: Sulfate aerosol indirect effect and co2 greenhouse forcing: Equilibrium response of the LMD GCM and associated cloud feedbacks, *J. Clim.*, 11(7), 1673–1684, 1998.

10   Lean, J.: Evolution of the sun's spectral irradiance since the maunder minimum, *Geophys. Res. Lett*, 27(16), 2425–2428, 2000

Lefevre, F., Brasseur, G., Folkins, I., Smith, A., and Simon, P.: Chemistry of the 1991–1992 stratospheric winter: Three-dimensional model simulations, *J. Geophys. Res.*, 99(D4), 8183–8195, 1994.

Lefèvre, F., Figarol, F., Carslaw, K.S., and Peter, T.: The 1997 arctic ozone depletion quantified from three-dimensional model simulations, *Geophys. Res. Lett*, 25(13), 2425–2428, 1998.

15   Lomb, N. R.: Least-squares frequency analysis of unequally spaced data, *Ap. Space Sci.*, 39(2), 447–462, 1976

Lott, F., Fairhead, L., Hourdin, F., and Levan, P.: The stratospheric version of LMDz: dynamical climatologies, arctic oscillation, and impact on the surface climate, *Clim. Dyn.*, 25(7-8), 851–868, 2005.

Madronich, S., and Flocke, S.: The role of solar radiation in atmospheric chemistry, in *Environmental photochemistry*, pp. 1–26, Springer, 1999.

20   Marchand, M., Keckhut, P., Lefebvre, S., Claud, C., Cugnet, D., Hauchecorne, A., Lefevre, F., Lefebvre, M.-P., Jumelet, J., Lott, F., Hourdin, F., Thuillier, G., Poulain, V., Bossay, S., Lemennais, P., David, C., and Bekki, S.: Dynamical amplification of the stratospheric solar response simulated with the Chemistry-Climate Model LMDz-Reprobus, *J. Atmos. Solar-Terr. Phys.*, 75–76, 147–160, 2012.

Maycock A. C., Matthes, K., Tegtmeier, S., Thiéblemont, R., and Hood, L.: The representation of solar cycle signals in

25   stratospheric ozone – Part 1: A comparison of satellite observations, *Atmos. Chem. Phys.*, doi:10.5194/acp-2015-882, 2016.

Meehl, G. A., Arblaster, J.M., Branstator, G., and van Loon, H.: A coupled air-sea response mechanism to solar forcing in the pacific region, *J. Clim.*, 21(12), 2883–2897, 2008.

Minschwaner, K., Anderson, G., Hall, L., and Yoshino, K.: Polynomial coefficients for calculating O_2 schumann-runge cross sections at 0.5 cm^{-1} resolution, *J. Geophys. Res.*, 97(D9), 10,103–10,108, 1992.

30   Morcrette, J.-J., Smith, L., and Fouquart, Y.: Pressure and temperature dependence of the absorption in longwave radiation parametrizations, *Beiträge zur Physik der Atmosphäre*, 59(4), 455–469, 1986.

Mudelsee, M.: *Climate Time Series Analysis: Classical Statistical and Bootstrap Methods*. Second edition. Springer, Cham Heidelberg New York Dordrecht London, 2014.

Poulain, V., Bekki, S., Marchand, M., Chipperfield, M.P., Khodri, M., Dhomse, S., Bodeker, G.E., Toumi, R., De Maziere, M., Pommereau, J.-P., Pazmino, A., Goutail, F., Plummer, D., Rozanov, E., Mancini, E., Akiyoshi, H., Lamarque, J.-F., and Austin, J.: Evaluation of the inter-annual variability of stratospheric chemical composition in chemistry-climate models using ground-based multi species time series, *J. Atmos. Sol-Terr. Phys.*, 145, Pages: 61-84, doi: 10.1016/j.jastp.2016.03.010, 2016.

5   Randel, W. J., and Wu, F.: A stratospheric ozone profile data set for 1979–2005: Variability, trends, and comparisons with column ozone data, *J. Geophys. Res.*, 112(D6), 2007.

Remsberg, E. E., Marshall, B. T., Garcia-Comas, M., Krueger, D., Lingenfelser, G. S., Martin-Torres, F. J., Mlynczak, M. G., Russell III, J. M., Smith, A. K., Zhao, Y., Brown, C. W., Gordley, L. L., Lopez-Gonzalez, M., Lopez-Puertas, M., She, C.-Y., Taylor, M. J., and Thompson, R. E.: Assessment of the quality of the Version 1.07 temperature versus pressure profiles of the

10   middle atmosphere from TIMED/SABER, *J. Geophys. Res.*, 113, D17101, doi:10.1029/2008JD010013, 2008.

Remsberg, E. E.: Decadal-scale responses in middle and upper stratospheric ozone from SAGE II version 7 data, *Atmos. Chem. Phys.*, 14, 1039–1053, doi:10.5194/acp-14-1039-2014, 2014.

Rottman, G., Woods, T., Snow, M., and DeToma, G.: The solar cycle variation in ultraviolet irradiance, *Adv. Space Res.*, 27, 1927{1932, doi:10.1016/S0273-1177(01)00272-1., 2001.

15   Rottman, G., Floyd, L., and Viereck, R.: Measurements of the solar ultraviolet irradiance, *Solar Variability and Its Effects on Climate*, pp. 111–125, 2004.

Rozanov, E., Egorova, T., Schmutz, W., and Peter, T.: Simulation of the stratospheric ozone and temperature response to the solar irradiance variability during sun rotation cycle, *J. Atmos. Solar-Terr. Phys.*, 68(18), 2203–2213, 2006

Sadourny, R., and Laval, K.: January and July performance of the LMD general circulation model, *New Perspectives in Climate*

20   *Modeling*, 1, 173–197, 1984.

Sander, S., Friedl, R.R., Barkern, J., Golden, D., Kurylo, M., Wine, P., Abbat, J., Burkholder, J., Moortgart, C., Huie, R., and Orkin, R. E.: Chemical kinetics and photochemical data for use in atmospheric studies, Technica Report, NASA/JPL Publication, California, USA, Evaluation No. 17, JPL Publication 10-6, 2011.

Savage, N., Law, K., Pyle, J., Richter, A., Nüß, H., and Burrows, J.: Using GOME n°2 satellite data to examine regional

25   differences in tomcat model performance, *Atmos. Chem. Phys.*, 4(7), 1895–1912, 2004.

Scargle, J. D.: Studies in astronomical time series analysis. ii-statistical aspects of spectral analysis of unevenly spaced data, *Astrophys. J.*, 263, 835–853, 1982.

Soukharev, B., and Hood, L.: Solar cycle variation of stratospheric ozone: Multiple regression analysis of long-term satellite data sets and comparisons with models, *J. Geophys. Res.*, 111(D20), 2006.

30   Stamnes, K., Tsay, S. Wiscombe, W., and Jayaweera, K.: A numerically stable algorithm for discrete-ordinate-method radiative transfer in multiple scattering and emitting layered media, *Appl. Opt.*, 27, 2502–2509, 1988.

Swartz, W. H., Stolarski, R.S., Oman, L.D., Fleming, E.L., and Jackman, C.H.: Middle atmosphere response to different descriptions of the 11-yr solar cycle in spectral irradiance in a chemistry-climate model, *Atmos. Chem. Phys.*, 12, 5937 5948, doi:10.5194/acp-12-5937-2012, 2012.

Atmospheric
Chemistry
and Physics
Discussions

Thuillier, G., Herse, M., Simon, P.C., Labs, D., Mandel, H., Gillotay, D., and Foujols, T.: The Visible Solar Spectral Irradiance from 350 to 850 NM as Measured by the SOLSPEC Spectrometer During the Atlas I Mission, *Solar Phys.*, 177, 41–61, 1998.

Torrence, C., and Compo, G.P.: A practical guide to wavelet analysis, *Bull. Am. Meteor. Soc.*, 79(1), 61–78, 1998.

Wang, Y.-M., Lean, J.L., and Sheeley, Jr N. R.: Modeling the Sun's magnetic field and irradiance since 1713. *Astrophys. J.* 625, 522–538, 2005.

Waters, J.: Microwave limb-sounding of Earth's upper atmosphere, *Atmos. Res.*, 23(3), 391–410, 1989.

Waters, J.: Microwave limb sounding, in *Atmospheric Remote Sensing by Microwave Radiometry*, vol. 1, p. 383, 1993.

Waters, J. W., Froidevaux, L., Harwood, R. S., Jarnot, R. F., Pickett, H. M., Read, W. G., Siegel, P. H., Cofield, R. E., Filipiak, M. J., Flower, D. A., Holden, J. R., Lau, G. K., Livesey, N. J., Manney, G. L., Pumphrey, H. C., Santee M. L., Wu, D. L., Cuddy, D.T., Lay, R. R., Loo, M. S., Perun, V. S., Schwartz, M. J., Stek, P. C., Thurstans, R. P., Boyles, M. A., Chandra, K. M., Chavez, M. C., Chen, G. S., Chudasama, B. V., Dodge, R., Fuller, R. A., Girard, M. A., Jiang, J. H., Jiang, Y. B., Knosp, B. W., LaBelle, R. C., Lam, J. C., Lee, K. A., Miller, D., Oswald, J. E., Patel, N.C., Pukala, D. M., Quintero, O., Scaff, D. M., Van Snyder, W., Tope, M. C., Wagner, P. A., and Walch, M. J.: The Earth Observing System Microwave Limb Sounder (EOS MLS) on the Aura satellite, *IEEE Transactions on Geoscience and Remote Sensing*, 44, 1075–1092, 2006.

Zhang, L., Cui, Y., He, Y., He, H., Du, Z., Li, R., and Wang, H.: Longitudinal distribution of major solar flares during 1975–2005, *Adv. Space Res.*, 40(7), 970–975, 2007.

Zhou, S., Miller, A.J., and Hood, L.L.: A partial correlation analysis of the stratospheric ozone response to 27-day solar UV variations with temperature effect removed, *J. Geophys. Res.*, 105(D4), 4491–4500, 2000.

Atmospheric
Chemistry
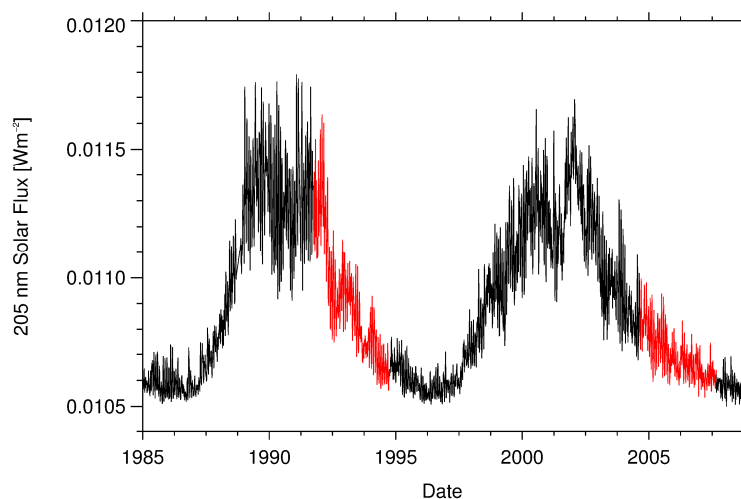and Physics
Discussions

Open Access

Figures

Figure 1: Temporal evolution of daily F205 from NRLSSI model over solar cycles 22 (1985-1996) and 23 (1996-2008). The two 3year periods considered here (1991-94 and 2004-07) are highlighted in red.
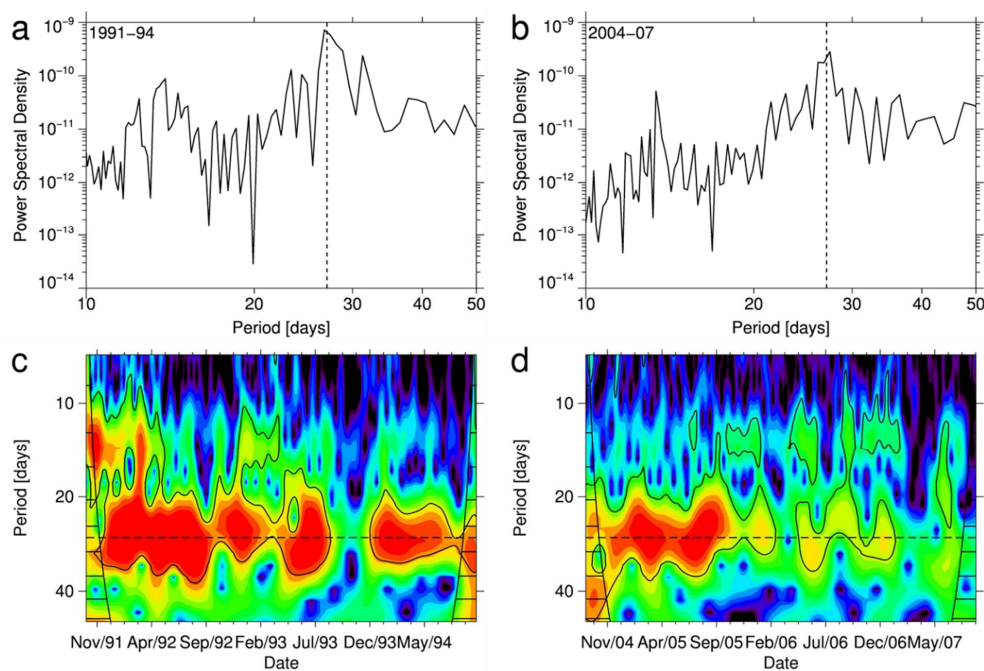
Atmospheric
Chemistry
and Physics
Discussions

Open Access

Figure 2: (Top) F205 FFT power spectra (from NRLSSI model) for the **(a)** 1991-94 and **(b)** 2004-07 period. **(Bottom)** Time-resolved power spectra densities (or scalogram) estimated from continuous wavelet transform (CWT) for the **(c)** 1991-94 and **(d)** 2004-07 period. The vertical, horizontal, dashed lines on (a,b), (c,d), indicate the 27day period. The cone of influence, i.e. limit beyond which scalogram should not be interpreted, is marked by horizontal solid stripes. The solid contour lines represent the 95% confidence level.

Figure 3: Ozone Lomb-Scargle periodograms for the (left) 1991-94 and (right) 2004-07 periods. The top panels represent ozone Lomb-Scargle periodograms from (a) MLS-UARS and (d) MLS-Aura observations. The middle panels (b and e) represent the ozone Lomb-Scargle periodograms for CTM simulation and the bottom panels (c and f) from the runs ensemble of the CCM simulations.
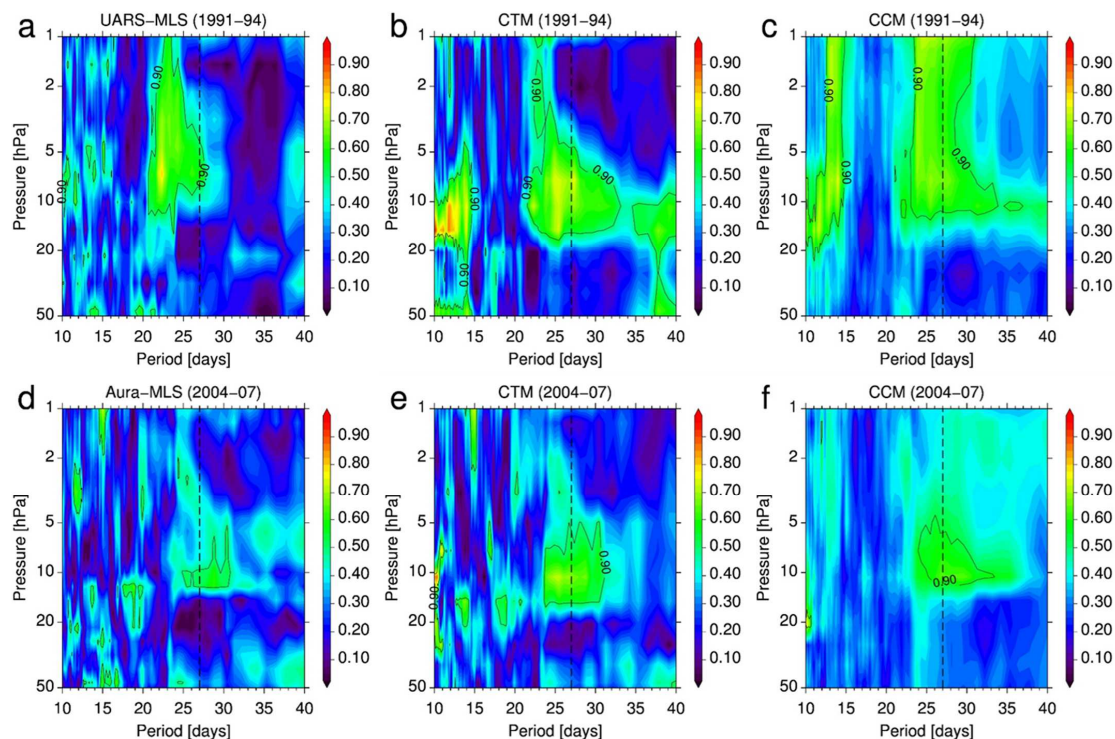5   **The dotted envelop (c and f) indicates the 2σ standard deviation of the ensemble of CCM simulations.**

Atmospheric
Chemistry
and Physics
Discussions

Open Access

EGU

Figure 4: Mean squared coherence between ozone and F205 as a function of period (days) and pressure level (hPa) for the (top) 1991-94 and (bottom) 2004-07 period and for (a, d) MLS observations, (b,e) CTM and (c,f) CCM simulations. Black contour lines indicate the 90% confidence level and the vertical dashed black lines indicate the 27day period.
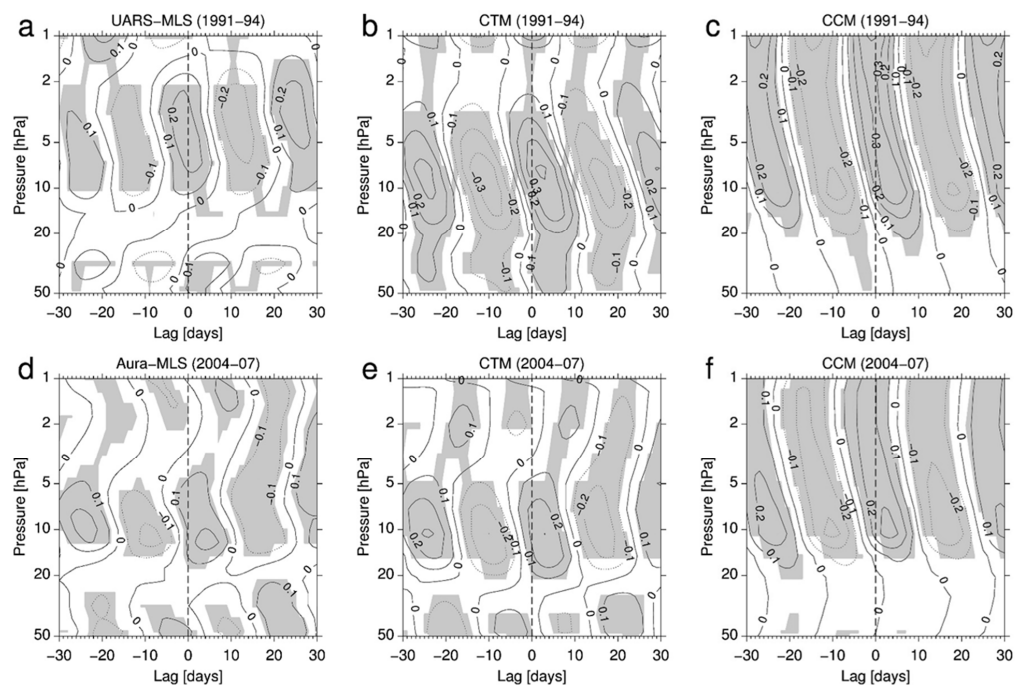
Figure 5: Cross-correlation between digitally filtered (see main text) ozone and F205 as a function of time lag (in days) and pressure level (hPa) for the (top) 1991-94 and (bottom) 2004-07 periods. (a,d), (b,e) and (c,f) panels show cross-correlation between F205 and MLS observations, CTM and CCM simulations, respectively. Shading represents areas with 95% confidence level.
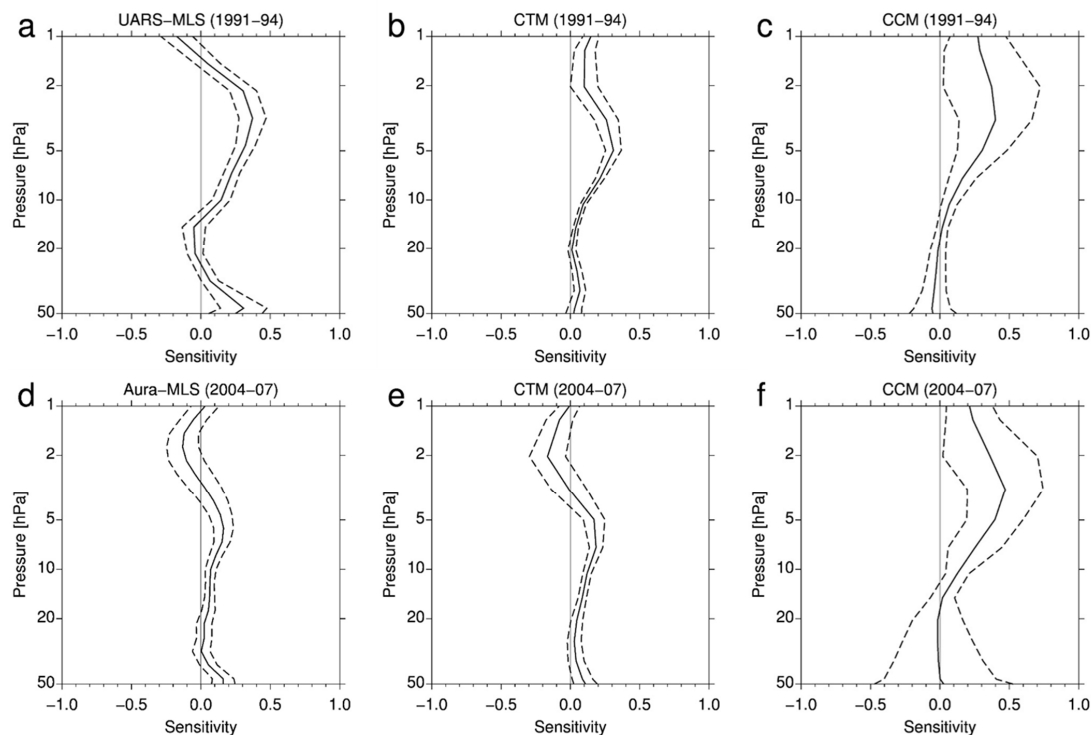
Atmospheric
Chemistry
and Physics
Discussions

Open Access

Figure 6: Vertical profile of ozone sensitivity to F205 (% change in ozone for 1% change in F205) at lag 0 for the (top) 1991-94 and (bottom) 2004-07 periods. Results are shown for (a) MLS-UARS, (d) MLS-Aura, (b, e) CTM simulations and (c,f) CCM ensemble simulations. (a,b,d,e) The dashed envelop indicates the 2σ standard error of the regression estimates. (c,f) The dashed envelop indicates the 2σ range.
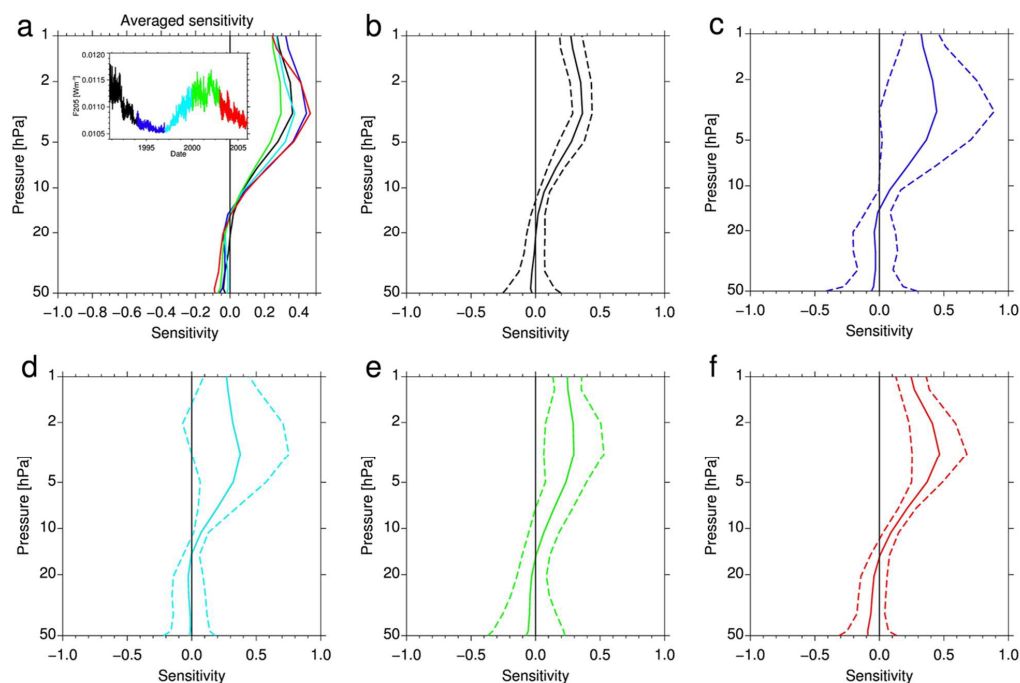
Atmospheric
Chemistry
and Physics
Discussions

Figure 7: (a) CCM ensemble ozone sensitivity profile for each of the 3year period. Each period and its corresponding colour is shown in the insert plot (a). CCM ensemble mean ozone sensitivity profile and its 2σ range are shown for each individual 3year periods: (b) 07/1990-06/1993, (c) 07/1993-06/1996, (d) 07/1996-06/1999, (e) 07/1999-06/2002, (f) 07/2002-06/2005.
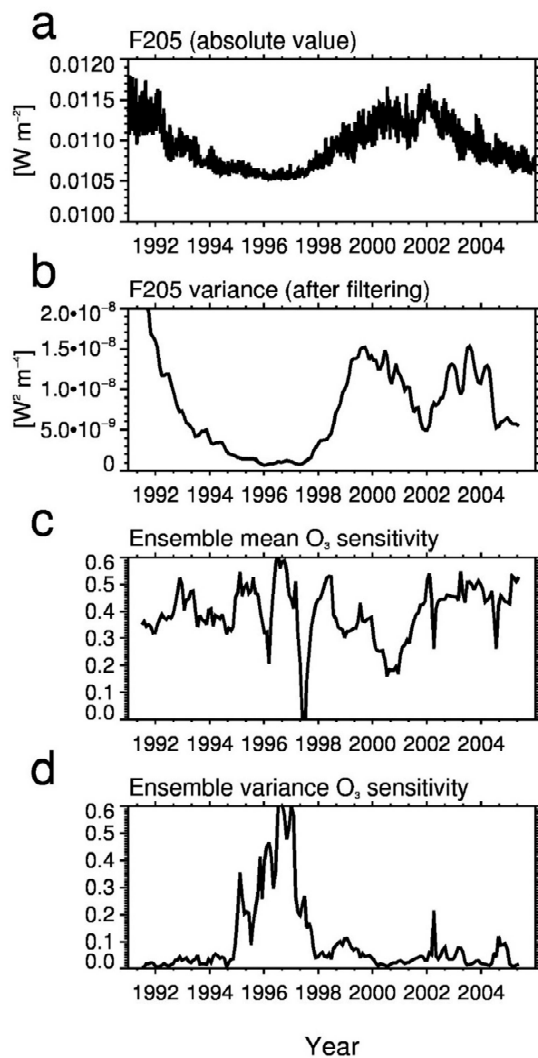
Figure 8: Digitally filtered (b) F205 variance time series, (c) ensemble mean ozone sensitivity and (d) ozone sensitivity ensemble variance time series at 3hPa computed over a 1year running window. Each window is sliding for one month at each step. (a) The F205 index time series is reproduced on the top panel for clarity.
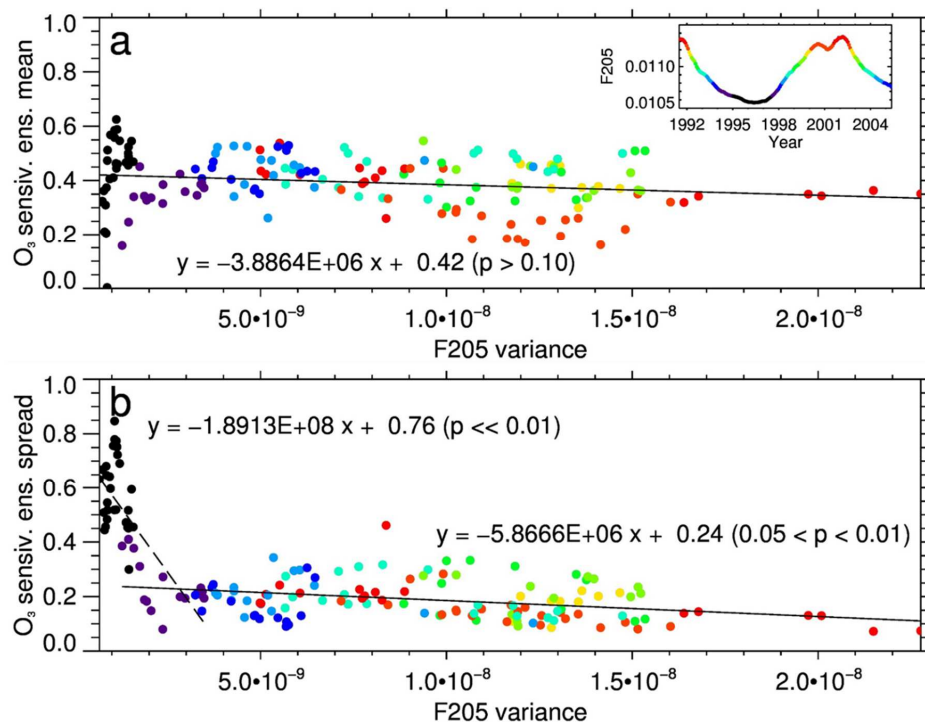
Figure 9: Scatter plots of the CCM ensemble (a) mean ozone sensitivity and (b) its spread (1σ) versus the F205 variance. Dots are coloured with respect to the value of the F205 flux, shown in the insert plot of panel a. Least square linear regression fits are superimposed (solid and dashed segments) together with their equation and the statistical significance of the slope value (in brackets, see text for details). The correlation coefficients are (a) -0.19 (p>0.10), (b, dashed) -0.76 (p<0.05) and (b, solid) -0.36 (p<0.10).

Atmospheric
Chemistry
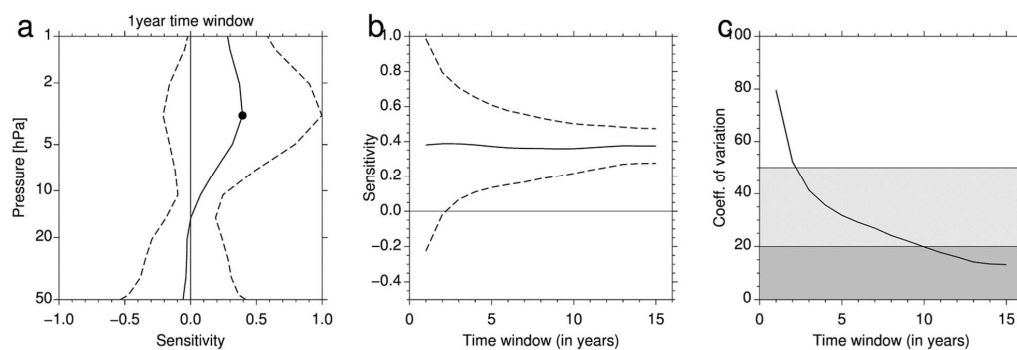and Physics

Open Access

EGU

Discussions

Figure 10: (a) CCM mean ozone sensitivity profile over the 1991-2005 period computed for a 1-year time window (see text for details on calculations). **(b)** Mean ozone sensitivity at 3 hPa (dot on (a)) as a function of the size of the time window. The dashed lines on (a) and (b) represent the 2σ spread. **(c)** Coefficient of variation (in %) of the ozone sensitivity as a function of the size of the time window. Intervals with values lower than 50% and 20% are highlighted by the gray shaded areas.